

Optimum Aerodynamic Design using the Navier–Stokes Equations

A. JAMESON^{*}, N.A. PIERCE[†] AND L. MARTINELLI[§]

^{*,§} *Department of Mechanical and Aerospace Engineering
Princeton University
Princeton, New Jersey 08544 USA*

and

[†] *Oxford University Computing Laboratory
Numerical Analysis Group
Oxford OX1 3QD UK*

35th AIAA Aerospace Sciences Meeting and Exhibit
Reno, NV, 1997

1 Introduction

The ultimate success of an aircraft design depends on the resolution of complex multi-disciplinary trade-offs between factors such as aerodynamic efficiency, structural weight, stability and control, and the volume required to contain fuel and payload. A design is finalized only after numerous iterations, cycling between the disciplines. The development of accurate and efficient methods for aerodynamic shape optimization represents a worthwhile intermediate step towards the eventual goal of full multi-disciplinary optimal design.

Early investigations into aerodynamic optimization relied on direct evaluation of the influence of each design variable. This dependence was estimated by separately varying each design parameter and recalculating the flow. The computational cost of this method is proportional to the number of design variables and consequently becomes prohibitive as the number of design parameters is increased.

An alternative approach to design relies on the fact that experienced designers generally have an intuitive feel for the type of pressure distribution that

will provide the desired aerodynamic performance. The resulting inverse problem amounts to determination of the shape corresponding to a specified pressure distribution. This approach has the advantage that only one flow solution is required to obtain the desired design. However, the problem must be formulated carefully to ensure that the target pressure distribution corresponds to a physically realizable shape.

The problems of optimal and inverse design can both be systematically treated within the mathematical theory for the control of systems governed by partial differential equations [1] by regarding the design problem as a control problem in which the control is the shape of the boundary. The inverse problem then becomes a special case of the optimal design problem in which the shape changes are driven by the discrepancy between the current and target pressure distributions.

The control theory approach to optimal aerodynamic design, in which shape changes are based on gradient information obtained by solution of an adjoint problem, was first applied to transonic flow by Jameson [2, 3]. He formulated the method for inviscid compressible flows with shocks governed by both the potential equation and the Euler equations [2, 4, 5]. With this approach, the cost of a design cycle is independent of the number of design vari-

^{*} James S. McDonnell Distinguished University Professor of Aerospace Engineering, AIAA Fellow

[†] Doctoral Candidate, Student Member AIAA

[§] Assistant Professor, Member AIAA

ables and the method has been employed for wing design in the context of complex aircraft configurations [6, 7], using a grid perturbation technique to accommodate the geometry modifications.

Ta’asan, Kuruvila and Salas have proposed a one shot approach in which the constraint represented by the flow equations need only be satisfied by the final converged design solution [8]. Pironneau has also studied the use of control theory for optimum shape design of systems governed by elliptic equations [9], and adjoint methods have also been used by Baysal and Eleshaky [10].

The objective of the present work is the extension of adjoint methods for optimal aerodynamic design to flows governed by the compressible Navier–Stokes equations. While inviscid formulations have proven useful for the design of transonic wings at cruise conditions, the inclusion of boundary layer displacement effects with viscous design provides increased realism and alleviates shocks that would otherwise form in the viscous solution over the final inviscid design. Accurate resolution of viscous effects such as separation and shock/boundary layer interaction is also essential for optimal design encompassing off-design conditions and high-lift configurations.

The computational costs of viscous design are at least an order of magnitude greater than for design using the Euler equations because a) the number of mesh points must be increased by a factor of two or more to resolve the boundary layer, b) there is the additional cost of computing the viscous terms and a turbulence model, and c) Navier–Stokes calculations generally converge much more slowly than Euler solutions due to stiffness arising from the highly stretched boundary layer cells. The computational feasibility of viscous design therefore hinges on the development of a rapidly convergent Navier–Stokes flow solver. Pierce and Giles have developed a preconditioned multigrid method that dramatically improves convergence of viscous calculations by ensuring that all error modes inside the stretched boundary layer cells are either damped or expelled [11, 12]. The same acceleration techniques are applicable to the adjoint calculation, so that a substantial reduction in the cost of each design cycle is achievable.

2 General Formulation of the Adjoint Approach to Optimal Design

Before embarking on a detailed derivation of the adjoint formulation for optimal design using the

Navier–Stokes equations, it is helpful to summarize the general abstract description of the adjoint approach which has been thoroughly documented in references [2, 3].

The progress of the design procedure is measured in terms of a cost function I , which could be, for example the drag coefficient or the lift to drag ratio. For flow about an airfoil or wing, the aerodynamic properties which define the cost function are functions of the flow-field variables (w) and the physical location of the boundary, which may be represented by the function \mathcal{F} , say. Then

$$I = I(w, \mathcal{F}),$$

and a change in \mathcal{F} results in a change

$$\delta I = \left[\frac{\partial I^T}{\partial w} \right]_I \delta w + \left[\frac{\partial I^T}{\partial \mathcal{F}} \right]_{II} \delta \mathcal{F}, \quad (1)$$

in the cost function. Here, the subscripts I and II are used to distinguish the contributions to the variation δw in the flow solution from the change associated directly with the modification $\delta \mathcal{F}$ in the shape. This notation is introduced to assist in grouping the plethora of terms that arise during the derivation of the full Navier–Stokes adjoint operator so that it remains feasible to recognize the basic structure of the approach as it is sketched in the present section.

Using control theory, the governing equations of the flow field are introduced as a constraint in such a way that the final expression for the gradient does not require multiple flow solutions. This corresponds to eliminating δw from (1).

Suppose that the governing equation R which expresses the dependence of w and \mathcal{F} within the flow-field domain D can be written as

$$R(w, \mathcal{F}) = 0. \quad (2)$$

Then δw is determined from the equation

$$\delta R = \left[\frac{\partial R}{\partial w} \right]_I \delta w + \left[\frac{\partial R}{\partial \mathcal{F}} \right]_{II} \delta \mathcal{F} = 0. \quad (3)$$

Next, introducing a Lagrange Multiplier ψ , we have

$$\delta I = \frac{\partial I^T}{\partial w} \delta w + \frac{\partial I^T}{\partial \mathcal{F}} \delta \mathcal{F} \quad (4)$$

$$- \psi^T \left(\left[\frac{\partial R}{\partial w} \right] \delta w + \left[\frac{\partial R}{\partial \mathcal{F}} \right] \delta \mathcal{F} \right) \quad (5)$$

$$= \left\{ \frac{\partial I^T}{\partial w} - \psi^T \left[\frac{\partial R}{\partial w} \right] \right\}_I \delta w \quad (6)$$

$$+ \left\{ \frac{\partial I^T}{\partial \mathcal{F}} - \psi^T \left[\frac{\partial R}{\partial \mathcal{F}} \right] \right\}_{II} \delta \mathcal{F}. \quad (7)$$

Choosing ψ to satisfy the adjoint equation

$$\left[\frac{\partial R}{\partial w} \right]^T \psi = \frac{\partial I}{\partial w} \quad (8)$$

the first term is eliminated, and we find that

$$\delta I = \mathcal{G} \delta \mathcal{F}, \quad (9)$$

where

$$\mathcal{G} = \frac{\partial I^T}{\partial \mathcal{F}} - \psi^T \left[\frac{\partial R}{\partial \mathcal{F}} \right].$$

The advantage is that (9) is independent of δw , with the result that the gradient of I with respect to an arbitrary number of design variables can be determined without the need for additional flow-field evaluations. In the case that (2) is a partial differential equation, the adjoint equation (8) is also a partial differential equation and determination of the appropriate boundary conditions requires careful mathematical treatment.

The computational cost of a single design cycle is roughly equivalent to the cost of two flow solutions since the the adjoint problem has similar complexity. When the number of design variables becomes large, the computational efficiency of the control theory approach over traditional approach, which requires direct evaluation of the gradients by individually varying each design variable and recomputing the flow field, becomes compelling.

Once equation (3) is established, an improvement can be made with a shape change

$$\delta \mathcal{F} = -\lambda \mathcal{G}$$

where λ is positive, and small enough that the first variation is an accurate estimate of δI . Then

$$\delta I = -\lambda \mathcal{G}^T \mathcal{G} < 0$$

After making such a modification, the gradient can be recalculated and the process repeated to follow a path of steepest descent until a minimum is reached. In order to avoid violating constraints, such as a minimum acceptable wing thickness, the gradient may be projected into an allowable subspace within which the constraints are satisfied. In this way, procedures can be devised which must necessarily converge at least to a local minimum.

3 The Navier–Stokes Equations

For the derivations that follow, it is convenient to adopt a Cartesian coordinate system defined by

(x_1, x_2, x_3) and to adopt the convention of indicial notation where a repeated index “ i ” implies summation over $i = 1$ to 3. The three-dimensional Navier–Stokes equations then take the form

$$\frac{\partial w}{\partial t} + \frac{\partial f_i}{\partial x_i} = \frac{\partial f_{vi}}{\partial x_i} \quad \text{in } \mathcal{D}, \quad (10)$$

where the state vector w , inviscid flux vector f and viscous flux vector f_v are described respectively by

$$w = \begin{Bmatrix} \rho \\ \rho u_1 \\ \rho u_2 \\ \rho u_3 \\ \rho E \end{Bmatrix}, \quad (11)$$

$$f_i = \begin{Bmatrix} \rho u_i \\ \rho u_i u_1 + p \delta_{i1} \\ \rho u_i u_2 + p \delta_{i2} \\ \rho u_i u_3 + p \delta_{i3} \\ \rho u_i H \end{Bmatrix}, \quad (12)$$

$$f_{vi} = \begin{Bmatrix} 0 \\ \sigma_{ij} \delta_{j1} \\ \sigma_{ij} \delta_{j2} \\ \sigma_{ij} \delta_{j3} \\ u_j \sigma_{ij} + k \frac{\partial T}{\partial x_i} \end{Bmatrix}. \quad (13)$$

In these definitions, ρ is the density, u_1, u_2, u_3 are the Cartesian velocity components, E is the total energy and δ_{ij} is the Kronecker delta function. The pressure is determined by the equation of state

$$p = (\gamma - 1) \rho \left\{ E - \frac{1}{2} (u_i u_i) \right\},$$

and the stagnation enthalpy is given by

$$H = E + \frac{p}{\rho},$$

where γ is the ratio of the specific heats. The viscous stresses may be written as

$$\sigma_{ij} = \mu \left(\frac{\partial u_i}{\partial x_j} + \frac{\partial u_j}{\partial x_i} \right) + \lambda \delta_{ij} \frac{\partial u_k}{\partial x_k},$$

where μ and λ are the first and second coefficients of viscosity and the coefficient of thermal conductivity and the temperature are defined by

$$k = \frac{\gamma \mu}{Pr}, \quad T = \frac{p}{(\gamma - 1) \rho}. \quad (14)$$

For discussion of real applications using a structured mesh discretization, it is also useful to consider

a transformation to the computational coordinates (ξ_1, ξ_2, ξ_3) defined by the metrics

$$K_{ij} = \left[\frac{\partial x_i}{\partial \xi_j} \right], \quad J = \det(K), \quad K_{ij}^{-1} = \left[\frac{\partial \xi_i}{\partial x_j} \right].$$

The Navier-Stokes equations can then be written in computational space as

$$\frac{\partial (Jw)}{\partial t} + \frac{\partial (F_i - F_{vi})}{\partial \xi_i} = 0 \quad \text{in } \mathcal{D}, \quad (15)$$

where the inviscid and viscous flux contributions are now defined with respect to the computational cell faces by $F_i = S_{ij} f_j$ and $F_{vi} = S_{ij} f_{vj}$, and the quantity $S_{ij} = JK_{ij}^{-1}$ is used to represent the projection of the ξ_i cell face along the x_j axis. In obtaining equation (15) we have made use of the property that

$$\frac{\partial S_{ij}}{\partial \xi_i} = 0 \quad (16)$$

which represents the fact that the sum of the face areas over a closed volume is zero, as can be readily verified by a direct examination of the metric terms.

General Formulation of the Optimal Design Problem for the Navier–Stokes Equations

Aerodynamic optimization is based on determination of the effect of shape modifications of the boundary on some performance measure which depends on the flow. For convenience, the coordinates ξ_i describing the fixed computational domain are chosen so that each boundary conforms to a constant value of one of these coordinates. Variations in the shape then result in corresponding variations in the mapping derivatives defined by K_{ij} .

Suppose that the performance is measured by a cost function

$$I = \int_{\mathcal{B}} \mathcal{M}(w, S) dB_{\xi} + \int_{\mathcal{D}} \mathcal{P}(w, S) dD_{\xi},$$

containing both boundary and field contributions where dB_{ξ} and dD_{ξ} are the surface and volume elements in the computational domain. In general, \mathcal{M} and \mathcal{P} will depend on both the flow variables w and the metrics S defining the computational space.

The design problem is now treated as a control problem where the wing shape represents the control function which is chosen to minimize I subject to the constraints defined by the flow equations (15).

A shape change produces a variation in the flow solution δw and the metrics δS which in turn produce a variation in the cost function

$$\delta I = \int_{\mathcal{B}} \delta \mathcal{M}(w, S) dB_{\xi} + \int_{\mathcal{D}} \delta \mathcal{P}(w, S) dD_{\xi}, \quad (17)$$

with

$$\begin{aligned} \delta \mathcal{M} &= [\mathcal{M}_w]_I \delta w + \delta \mathcal{M}_{II}, \\ \delta \mathcal{P} &= [\mathcal{P}_w]_I \delta w + \delta \mathcal{P}_{II}, \end{aligned} \quad (18)$$

where we continue to use the subscripts I and II to distinguish between the contributions associated with the variation of the flow solution δw and those associated with the metric variations δS . Thus $[\mathcal{M}_w]_I$ and $[\mathcal{P}_w]_I$ represent $\frac{\partial \mathcal{M}}{\partial w}$ and $\frac{\partial \mathcal{P}}{\partial w}$ with the metrics fixed, while $\delta \mathcal{M}_{II}$ and $\delta \mathcal{P}_{II}$ represent the contribution of the metric variations δS to $\delta \mathcal{M}$ and $\delta \mathcal{P}$.

In the steady state, the constraint equation (15) specifies the variation of the state vector δw by

$$\frac{\partial}{\partial \xi_i} \delta (F_i - F_{vi}) = 0. \quad (19)$$

Here δF_i and δF_{vi} can also be split into contributions associated with δw and δS using the notation

$$\begin{aligned} \delta F_i &= [F_{iw}]_I \delta w + \delta F_{iII} \\ \delta F_{vi} &= [F_{v iw}]_I \delta w + \delta F_{viII}. \end{aligned} \quad (20)$$

The inviscid contributions are easily evaluated as

$$[F_{iw}]_I = S_{ij} \frac{\partial f_i}{\partial w}, \quad \delta F_{viII} = \delta S_{ij} f_j.$$

The details of the viscous contributions are complicated by the additional level of derivatives in the stress and heat flux terms and will be derived in Section 5. Multiplying by a co-state vector ψ , which will play an analogous role to the Lagrange multiplier introduced in equation (7), and integrating over the domain produces

$$\int_{\mathcal{D}} \psi^T \frac{\partial}{\partial \xi_i} \delta (F_i - F_{vi}) = 0. \quad (21)$$

If ψ is differentiable this may be integrated by parts to give

$$\int_{\mathcal{B}} n_i \psi^T \delta (F_i - F_{vi}) dB_{\xi} \quad (22)$$

$$- \int_{\mathcal{D}} \frac{\partial \psi^T}{\partial \xi_i} \delta (F_i - F_{vi}) dD_{\xi} = 0. \quad (23)$$

Since the left hand expression equals zero, it may be subtracted from the variation in the cost function

(17) to give

$$\begin{aligned} \delta I &= \int_{\mathcal{B}} [\delta \mathcal{M} - n_i \psi^T \delta (F_i - F_{vi})] d\mathcal{B}_\xi \\ &+ \int_{\mathcal{D}} \left[\delta \mathcal{P} + \frac{\partial \psi^T}{\partial \xi_i} \delta (F_i - F_{vi}) \right] d\mathcal{D}_\xi. \end{aligned} \quad (24)$$

Now, since ψ is an arbitrary differentiable function, it may be chosen in such a way that δI no longer depends explicitly on the variation of the state vector δw . The gradient of the cost function can then be evaluated directly from the metric variations without having to recompute the variation δw resulting from the perturbation of each design variable.

Comparing equations (18) and (20), the variation δw may be eliminated from (24) by equating all field terms with subscript “ I ” to produce a differential adjoint system governing ψ

$$\frac{\partial \psi^T}{\partial \xi_i} [F_{j_w} - F_{v_{j_w}}]_I + \mathcal{P}_w = 0 \quad \text{in } \mathcal{D}. \quad (25)$$

The corresponding adjoint boundary condition is produced by equating the subscript “ I ” boundary terms in equation (24) to produce

$$n_i \psi^T [F_{j_w} - F_{v_{j_w}}]_I = \mathcal{M}_w \quad \text{on } \mathcal{B}. \quad (26)$$

The remaining terms from equation (24) then yield a simplified expression for the variation of the cost function which defines the gradient

$$\begin{aligned} \delta I &= \int_{\mathcal{B}} \{ \delta \mathcal{M}_I - n_i \psi^T (F_i - F_{vi}) \} d\mathcal{B}_\xi \\ &+ \int_{\mathcal{D}} \{ \delta \mathcal{P}_I + [\delta F_i - \delta F_{vi}]_I \} d\mathcal{D}_\xi, \end{aligned} \quad (27)$$

The details of the formula for the gradient depend on the way in which the boundary shape is parameterized as a function of the design variables and the way in which the mesh is deformed as the boundary is modified. Using the relationship between the mesh deformation and the surface modification, the field integral is reduced to a surface integral by integrating along the coordinate lines emanating from the surface. Thus the expression for δI is finally reduced to the form of equation (9)

$$\delta I = \int_{\mathcal{B}} \mathcal{G} \delta S d\mathcal{B}_\xi$$

where S represents the design variables, and \mathcal{G} is the gradient, which is a function defined over the boundary surface.

The boundary conditions satisfied by the flow equations restrict the form of the left hand side of

the adjoint boundary condition (26). Consequently, the boundary contribution to the cost function \mathcal{M} cannot be specified arbitrarily. Instead, it must be chosen from the class of functions which allow cancellation of all terms containing δw in the boundary integral of equation (24). On the other hand, there is no such restriction on the specification of the field contribution to the cost function \mathcal{P} , since these terms may always be absorbed into the adjoint field equation (25) as source terms.

It is convenient to develop the inviscid and viscous contributions to the adjoint equation separately. Also, for simplicity, it will be assumed that the portion of the boundary that undergoes shape modifications is restricted to the coordinate surface $\xi_2 = 0$. Then equations (24) and (26) may be simplified by incorporating the conditions

$$n_1 = n_3 = 0, \quad n_2 = 1, \quad d\mathcal{B}_\xi = d\xi_1 d\xi_3,$$

so that only the variations δF_2 and δF_{v_2} need to be considered at the wall boundary.

4 Derivation of the Inviscid Adjoint Terms

The inviscid contributions have been previously derived in [4, 13] but are included here for completeness. Taking the transpose of equation (25), the inviscid adjoint equation may be written as

$$C_i^T \frac{\partial \psi}{\partial \xi_i} = 0 \quad \text{in } \mathcal{D}, \quad (28)$$

where the inviscid Jacobian matrices in the transformed space are given by

$$C_i = S_{ij} \frac{\partial f_j}{\partial w}.$$

The transformed velocity components have the form

$$U_i = S_{ij} u_j,$$

and the condition that there is no flow through the wall boundary at $\xi_2 = 0$ is equivalent to

$$U_2 = 0,$$

so that

$$\delta U_2 = 0$$

when the boundary shape is modified. Consequently the variation of the inviscid flux at the boundary reduces to

$$\delta F_2 = \delta p \begin{pmatrix} 0 \\ S_{2j} \\ S_{22} \\ S_{23} \\ 0 \end{pmatrix} + p \begin{pmatrix} 0 \\ \delta S_{2j} \\ \delta S_{22} \\ \delta S_{23} \\ 0 \end{pmatrix}. \quad (29)$$

Since δF_2 depends only on the pressure, it is now clear that the performance measure on the boundary $\mathcal{M}(w, S)$ may only be a function of the pressure and metric terms. Otherwise, complete cancellation of the terms containing δw in the boundary integral would be impossible. One may, for example, include arbitrary measures of the forces and moments in the cost function, since these are functions of the surface pressure.

In order to design a shape which will lead to a desired pressure distribution a natural choice is to set

$$I = \frac{1}{2} \int_B (p - p_d)^2 dS$$

where p_d is the desired surface pressure, and the integral is evaluated over the actual surface area. In the computational domain this is transformed to

$$I = \frac{1}{2} \iint_{B_w} (p - p_d)^2 |S_2| d\xi_1 d\xi_3,$$

where the quantity

$$|S_2| = \sqrt{S_{2j} S_{2j}}$$

denotes the face area corresponding to a unit element of face area in the computational domain. Now, to cancel the dependence of the boundary integral on δp , the adjoint boundary condition reduces to

$$\psi_j n_j = p - p_d \quad (30)$$

where n_j are the components of the surface normal

$$n_j = \frac{S_{2j}}{|S_2|}.$$

This amounts to a transpiration boundary condition on the co-state variables corresponding to the momentum components. Note that it imposes no restriction on the tangential component of ψ at the boundary.

In the presence of shock waves, neither p nor p_d are necessarily continuous at the surface. The boundary condition is then in conflict with the assumption that ψ is differentiable. This difficulty can be circumvented by the use of a smoothed boundary condition [13].

5 Derivation of the Viscous Adjoint Terms

In computational coordinates the viscous terms in the Navier–Stokes equations have the form

$$\frac{\partial F_{vi}}{\partial \xi_i} = \frac{\partial}{\partial \xi_i} (S_{ij} f_{vj}).$$

Computing the variation δw resulting from a shape modification of the boundary, introducing a co-state vector ψ and integrating by parts following the steps outlined by equations (19) to (23) produces

$$\begin{aligned} & \int_B \psi^T (\delta S_{2j} f_{vj} + S_{2j} \delta f_{vj}) d\mathcal{B}_\xi \\ & - \int_D \frac{\partial \psi^T}{\partial \xi_i} (\delta S_{ij} f_{vj} + S_{ij} \delta f_{vj}) d\mathcal{D}_\xi, \end{aligned}$$

where the wall is defined by the coordinate surface $\xi_2 = 0$ so that $n_1 = n_3 = 0$, and $n_2 = 1$. Furthermore, it is assumed that the boundary contributions at the far field may either be neglected or else eliminated by a proper choice of boundary conditions as previously shown for the inviscid case [4, 13].

Transformation to Primitive Variables

The derivation of the viscous adjoint terms is simplified by transforming to the primitive variables

$$\tilde{w}^T = (\rho, u, v, w, p)^T.$$

because the viscous stresses depend on the velocity derivatives $\frac{\partial u_i}{\partial x_j}$, while the heat fluxes can be expressed as

$$k \frac{\partial}{\partial x_i} \left(\frac{p}{\rho} \right).$$

The relationship between the conservative and primitive variations are defined by the expressions

$$\delta w = M \delta \tilde{w}, \quad \delta \tilde{w} = M^{-1} \delta w$$

which make use of the transformation matrices $M = \frac{\partial w}{\partial \tilde{w}}$ and $M^{-1} = \frac{\partial \tilde{w}}{\partial w}$. These matrices are provided in transposed form for future convenience

$$M^T = \begin{bmatrix} 1 & u_1 & u_2 & u_3 & \frac{u_i u_i}{2} \\ 0 & \rho & 0 & 0 & \rho u_1 \\ 0 & 0 & \rho & 0 & \rho u_2 \\ 0 & 0 & 0 & \rho & \rho u_3 \\ 0 & 0 & 0 & 0 & \frac{1}{\gamma-1} \end{bmatrix}$$

$$M^{-1T} = \begin{bmatrix} 1 & -\frac{u_1}{\rho} & -\frac{u_2}{\rho} & -\frac{u_3}{\rho} & \frac{(\gamma-1)u_i u_i}{2} \\ 0 & \frac{1}{\rho} & 0 & 0 & -(\gamma-1)u_1 \\ 0 & 0 & \frac{1}{\rho} & 0 & -(\gamma-1)u_2 \\ 0 & 0 & 0 & \frac{1}{\rho} & -(\gamma-1)u_3 \\ 0 & 0 & 0 & 0 & \gamma-1 \end{bmatrix}.$$

The conservative and primitive adjoint operators L and \tilde{L} corresponding to the variations δw and $\delta \tilde{w}$ are then related by

$$\int_{\mathcal{D}} \delta w^T L \psi \, d\mathcal{D}_\xi = \int_{\mathcal{D}} \delta \tilde{w}^T \tilde{L} \psi \, d\mathcal{D}_\xi,$$

with

$$\tilde{L} = M^T L,$$

so that after determining the primitive adjoint operator by direct evaluation of the viscous portion of (25), the conservative operator may be obtained by the transformation $L = M^{-1T} \tilde{L}$. There is no contribution from the continuity equation so the derivation proceeds by first examining the adjoint operators arising from the momentum equations.

Contributions from the Momentum Equations

In order to make use of the summation convention, it is convenient to set $\psi_{j+1} = \phi_j$ for $j = 1, 2, 3$. Then the contribution from the momentum equations is

$$\begin{aligned} & \int_{\mathcal{B}} \phi_k (\delta S_{2j} \sigma_{kj} + S_{2j} \delta \sigma_{kj}) \, d\mathcal{B}_\xi \\ & - \int_{\mathcal{D}} \frac{\partial \phi_k}{\partial \xi_i} (\delta S_{ij} \sigma_{kj} + S_{ij} \delta \sigma_{kj}) \, d\mathcal{D}_\xi. \end{aligned} \quad (31)$$

The velocity derivatives in the viscous stresses can be expressed as

$$\frac{\partial u_i}{\partial x_j} = \frac{\partial u_i}{\partial \xi_l} \frac{\partial \xi_l}{\partial x_j} = \frac{S_{lj}}{J} \frac{\partial u_i}{\partial \xi_l}$$

with corresponding variations

$$\delta \frac{\partial u_i}{\partial x_j} = \left[\frac{\partial u_i}{\partial \xi_l} \right]_I \delta \left(\frac{S_{lj}}{J} \right) + \left[\frac{S_{lj}}{J} \right]_{II} \frac{\partial}{\partial \xi_l} \delta u_i.$$

The variation in the stresses are then

$$\begin{aligned} \delta \sigma_{kj} &= \left\{ \mu \left[\frac{S_{lj}}{J} \frac{\partial}{\partial \xi_l} \delta u_k + \frac{S_{lk}}{J} \frac{\partial}{\partial \xi_l} \delta u_j \right] \right. \\ &\quad \left. + \lambda \left[\delta_{jk} \frac{S_{lm}}{J} \frac{\partial}{\partial \xi_l} \delta u_m \right] \right\}_I \\ &+ \left\{ \mu \left[\delta \left(\frac{S_{lj}}{J} \right) \frac{\partial u_k}{\partial \xi_l} + \delta \left(\frac{S_{lk}}{J} \right) \frac{\partial u_j}{\partial \xi_l} \right] \right. \\ &\quad \left. + \lambda \left[\delta_{jk} \delta \left(\frac{S_{lm}}{J} \right) \frac{\partial u_m}{\partial \xi_l} \right] \right\}_{II}. \end{aligned}$$

The metric variations with subscript II that arise in this expression are among those whose absence was alluded to with regard to equation (20). Since these terms have no dependence on variations in the flow field δw , they do not contribute to the viscous adjoint operator, but instead yield an additional metric

variation term in the field contribution to the variation of the cost function in equation (27). Therefore, only those terms with subscript I need be considered further in deriving the viscous adjoint operator. The field contributions that contain δu_i in equation (31) appear as

$$\begin{aligned} & - \int_{\mathcal{D}} \frac{\partial \phi_k}{\partial \xi_i} S_{ij} \left\{ \mu \left(\frac{S_{lj}}{J} \frac{\partial}{\partial \xi_l} \delta u_k + \frac{S_{lk}}{J} \frac{\partial}{\partial \xi_l} \delta u_j \right) \right. \\ &\quad \left. + \lambda \delta_{jk} \frac{S_{lm}}{J} \frac{\partial}{\partial \xi_l} \delta u_m \right\} \, d\mathcal{D}_\xi. \end{aligned}$$

This may be integrated by parts to yield

$$\begin{aligned} & \int_{\mathcal{D}} \delta u_k \frac{\partial}{\partial \xi_l} \left(S_{lj} S_{ij} \frac{\mu}{J} \frac{\partial \phi_k}{\partial \xi_i} \right) \, d\mathcal{D}_\xi \\ & + \int_{\mathcal{D}} \delta u_j \frac{\partial}{\partial \xi_l} \left(S_{lk} S_{ij} \frac{\mu}{J} \frac{\partial \phi_k}{\partial \xi_i} \right) \, d\mathcal{D}_\xi \\ & + \int_{\mathcal{D}} \delta u_m \frac{\partial}{\partial \xi_l} \left(S_{lm} S_{ik} \frac{\lambda \delta_{jk}}{J} \frac{\partial \phi_k}{\partial \xi_i} \right) \, d\mathcal{D}_\xi, \end{aligned}$$

where the boundary integral has been eliminated by noting that $\delta u_i = 0$. By exchanging indices, the field integrals may be combined to produce

$$\begin{aligned} & \int_{\mathcal{D}} \delta u_k \frac{\partial}{\partial \xi_l} S_{ij} \left\{ \mu \left(\frac{S_{ij}}{J} \frac{\partial \phi_k}{\partial \xi_j} + \frac{S_{ik}}{J} \frac{\partial \phi_j}{\partial \xi_k} \right) \right. \\ &\quad \left. + \lambda \delta_{jk} \frac{S_{im}}{J} \frac{\partial \phi_m}{\partial \xi_l} \right\} \, d\mathcal{D}_\xi, \end{aligned}$$

which is further simplified by transforming the inner derivatives back to Cartesian coordinates

$$\int_{\mathcal{D}} \delta u_k \frac{\partial}{\partial \xi_l} S_{ij} \left\{ \mu \left(\frac{\partial \phi_k}{\partial x_j} + \frac{\partial \phi_j}{\partial x_k} \right) + \lambda \delta_{jk} \frac{\partial \phi_m}{\partial x_m} \right\} \, d\mathcal{D}_\xi. \quad (32)$$

The boundary contributions that contain δu_i in equation (31) may be simplified using the fact that

$$\frac{\partial}{\partial \xi_l} \delta u_i = 0 \quad \text{if } l = 1, 3$$

on the boundary \mathcal{B} so that they become

$$\begin{aligned} & \int_{\mathcal{B}} \phi_k S_{2j} \left\{ \mu \left(\frac{S_{2j}}{J} \frac{\partial}{\partial \xi_2} \delta u_k + \frac{S_{2k}}{J} \frac{\partial}{\partial \xi_2} \delta u_j \right) \right. \\ &\quad \left. + \lambda \delta_{jk} \frac{S_{2m}}{J} \frac{\partial}{\partial \xi_2} \delta u_m \right\} \, dS_x. \end{aligned} \quad (33)$$

Together, (32) and (33) comprise the field and boundary contributions of the momentum equations to the viscous adjoint operator in primitive variables.

Contributions from the Energy Equation

In order to derive the contribution of the energy equation to the viscous adjoint terms it is convenient

to set

$$\psi_5 = \Phi, \quad Q_j = u_i \sigma_{ij} + \frac{k}{\gamma - 1} \frac{\partial}{\partial x_j} \left(\frac{p}{\rho} \right),$$

where the temperature has been written in terms of pressure and density using (14). The contribution from the energy equation can then be written as

$$\begin{aligned} & \int_{\mathcal{B}} \Phi (\delta S_{2j} Q_j + S_{2j} \delta Q_j) d\mathcal{B}_\xi \\ & - \int_{\mathcal{D}} \frac{\partial \Phi}{\partial \xi_i} (\delta S_{ij} Q_j + S_{ij} \delta Q_j) d\mathcal{D}_\xi. \end{aligned} \quad (34)$$

The field contributions that contain $\delta u_i, \delta p$, and $\delta \rho$ in equation (34) appear as

$$\begin{aligned} & - \int_{\mathcal{D}} \frac{\partial \Phi}{\partial \xi_i} S_{ij} \delta Q_j d\mathcal{D}_\xi = \\ & - \int_{\mathcal{D}} \frac{\partial \Phi}{\partial \xi_i} S_{ij} \{ \delta u_k \sigma_{kj} + u_k \delta \sigma_{kj} \\ & + \frac{k}{\gamma - 1} \frac{S_{lj}}{J} \frac{\partial}{\partial \xi_l} \left(\frac{\delta p}{\rho} - \frac{p \delta \rho}{\rho} \right) \} d\mathcal{D}_\xi. \end{aligned} \quad (35)$$

The term involving $\delta \sigma_{kj}$ may be integrated by parts to produce

$$\begin{aligned} & \int_{\mathcal{D}} \delta u_k \frac{\partial}{\partial \xi_l} S_{lj} \left\{ \mu \left(u_k \frac{\partial \Phi}{\partial x_j} + u_j \frac{\partial \Phi}{\partial x_k} \right) \right. \\ & \left. + \lambda S_{ik} u_m \frac{\partial \Phi}{\partial x_m} \right\} d\mathcal{D}_\xi \end{aligned} \quad (36)$$

where the conditions $u_i = \delta u_i = 0$ are used to eliminate the boundary integral on \mathcal{B} . Notice that the other term in (35) that involves δu_k need not be integrated by parts and is merely carried on as

$$- \int_{\mathcal{D}} \delta u_k \sigma_{kj} S_{ij} \frac{\partial \Phi}{\partial \xi_i} d\mathcal{D}_\xi \quad (37)$$

The terms in expression (35) that involve δp and $\delta \rho$ may also be integrated by parts to produce both a field and a boundary integral. The field integral becomes

$$\int_{\mathcal{D}} \left(\frac{\delta p}{\rho} - \frac{p \delta \rho}{\rho} \right) \frac{\partial}{\partial \xi_l} \left(S_{lj} S_{ij} \frac{k}{(\gamma - 1) J} \frac{\partial \Phi}{\partial \xi_i} \right) d\mathcal{D}_\xi$$

which may be simplified by transforming the inner derivative to Cartesian coordinates

$$\int_{\mathcal{D}} \left(\frac{\delta p}{\rho} - \frac{p \delta \rho}{\rho} \right) \frac{\partial}{\partial \xi_l} \left(S_{lj} \frac{k}{\gamma - 1} \frac{\partial \Phi}{\partial x_j} \right) d\mathcal{D}_\xi. \quad (38)$$

The boundary integral becomes

$$\int_{\mathcal{B}} \frac{k}{\gamma - 1} \left(\frac{\delta p}{\rho} - \frac{p \delta \rho}{\rho} \right) \frac{S_{2j} S_{ij}}{J} \frac{\partial \Phi}{\partial \xi_i} d\mathcal{B}_\xi \quad (39)$$

which can also be simplified by transforming the inner derivative to Cartesian coordinates

$$\int_{\mathcal{B}} \frac{k}{\gamma - 1} \left(\frac{\delta p}{\rho} - \frac{p \delta \rho}{\rho} \right) \frac{S_{2j}}{J} \frac{\partial \Phi}{\partial x_j} d\mathcal{B}_\xi, \quad (40)$$

and identifying the normal derivative at the wall

$$\frac{\partial}{\partial n} = S_{2j} \frac{\partial}{\partial x_j} \quad (41)$$

and the variation in temperature

$$\delta T = \frac{k}{\gamma - 1} \left(\frac{\delta p}{\rho} - \frac{p \delta \rho}{\rho} \right)$$

to produce the boundary contribution

$$\int_{\mathcal{B}} k \delta T \frac{\partial \Phi}{\partial n} d\mathcal{B}_\xi. \quad (42)$$

This term vanishes if T is constant on the wall but persists if the wall is adiabatic.

There is also a boundary contribution left over from the first integration by parts (34) which has the form

$$\int_{\mathcal{B}} \Phi \delta (S_{2j} Q_j) d\mathcal{B}_\xi \quad (43)$$

where

$$Q_j = k \frac{\partial T}{\partial x_j}$$

since $u_i = 0$. Notice that for future convenience in discussing the adjoint boundary conditions resulting from the energy equation, both the δw and δS terms corresponding to subscript classes *I* and *II* are considered simultaneously. If the wall is adiabatic

$$\frac{\partial T}{\partial n} = 0$$

so that using (41)

$$\delta (S_{2j} Q_j) = 0$$

and both the δw and δS boundary contributions vanish.

On the other hand, if T is constant then it is more convenient to expand (43) into

$$\int_{\mathcal{B}} \Phi (\delta S_{2j} Q_j + S_{2j} \delta Q_j) d\mathcal{B}_\xi$$

where, since $\frac{\partial T}{\partial \xi_i} = 0$ for $l = 1, 3$,

$$\delta Q_j = k \delta \frac{\partial T}{\partial x_j} = k \delta \left(\frac{S_{lj}}{J} \frac{\partial T}{\partial \xi_l} \right) = k \delta \left(\frac{S_{2j}}{J} \frac{\partial T}{\partial \xi_2} \right)$$

so that the boundary integral (43) becomes

$$\int_{\mathcal{B}} \Phi \left\{ \frac{S_{2j}}{J} \frac{\partial}{\partial \xi_2} \delta T + k \left[\delta \left(S_{2j} + \frac{S_{2j}}{J} \right) \frac{\partial T}{\partial \xi_l} \right] \right\} d\mathcal{B}_\xi \quad (44)$$

Therefore, for constant T , the first term corresponding to variations in the flow field contributes to the adjoint boundary operator and the second set of terms corresponding to metric variations contribute to the cost function gradient.

All together, the contributions from the energy equation to the viscous adjoint operator are the three field terms (36), (37) and (38), and either of two boundary contributions, depending on whether the wall is adiabatic (42) or has constant temperature (42).

6 The Viscous Adjoint Field Operator

Collecting together the contributions from the momentum and energy equations, the viscous adjoint operator in primitive variables can be expressed as

$$\begin{aligned} (\tilde{L}\psi)_1 &= -\frac{p}{(\gamma-1)\rho^2} \frac{\partial}{\partial \xi_l} \left(S_{lj} k \frac{\partial \Phi}{\partial x_j} \right) \\ (\tilde{L}\phi)_i &= \frac{\partial}{\partial \xi_l} \left\{ S_{lj} \left[\mu \left(\frac{\partial \phi_i}{\partial x_j} + \frac{\partial \phi_j}{\partial x_i} \right) + \lambda \delta_{ij} \frac{\partial \phi_k}{\partial x_k} \right] \right\} \\ &+ \frac{\partial}{\partial \xi_l} \left\{ S_{lj} \left[\mu \left(\frac{\partial \Phi}{\partial x_j} + \frac{\partial \Phi}{\partial x_i} \right) + \lambda \delta_{ij} \frac{\partial \Phi}{\partial x_k} \right] \right\} \\ &- \sigma_{ij} S_{lj} \frac{\partial \Phi}{\partial x_l} \\ (\tilde{L}\Phi) &= \frac{\rho}{(\gamma-1)} \frac{\partial}{\partial \xi_l} \left(S_{lj} k \frac{\partial \Phi}{\partial x_j} \right), \end{aligned}$$

so that the conservative viscous adjoint operator may be obtained by the transformation

$$L = M^{-1T} \tilde{L}.$$

7 Viscous Adjoint Boundary Conditions

As previously noted, the boundary conditions satisfied by the flow equations restrict the form of the performance measure that may be chosen for the cost function. There must be a direct correspondence between the flow variables for which variations appear in the expression for the cost function gradient and those variables for which variations appear

in the boundary terms arising during the derivation of the adjoint field equations. Otherwise it would be impossible to eliminate the dependence of δI on δw through proper specification of the adjoint boundary condition. As in the derivation of the field equations, it proves convenient to consider the contributions from the momentum equations and the energy equation separately.

Boundary Conditions Arising from the Momentum Equations

The boundary term that arises from the momentum equations including both the δw and δS components (31) takes the form

$$\int_{\mathcal{B}} \phi_k \delta (S_{2j} \sigma_{kj}) d\mathcal{B}_\xi.$$

Replacing the metric term with the corresponding local face area S_2 and unit normal n_j defined by

$$|S_2| = \sqrt{S_{2j} S_{2j}}, \quad n_j = \frac{S_{2j}}{|S_2|}$$

then leads to

$$\int_{\mathcal{B}} \phi_k \delta (|S_2| n_j \sigma_{kj}) d\mathcal{B}_\xi.$$

Defining the components of the surface stress as

$$\tau_k = n_j \sigma_{kj}$$

and the physical surface element

$$dS = |S_2| d\mathcal{B}_\xi,$$

the integral may then be split into two components

$$\int_{\mathcal{B}} \phi_k \tau_k |\delta S_2| d\mathcal{B}_\xi + \int_{\mathcal{B}} \phi_k |S_2| \delta \tau_k dS, \quad (45)$$

where only the second term contains variations in the flow variables and must consequently cancel the δw terms arising in the cost function. The first term will appear in the expression for the cost function gradient.

A general form of the cost function that allows cancellation with terms containing $\delta \tau_k$ has the form

$$I = \int_{\mathcal{B}} \mathcal{N}(\tau) dS, \quad (46)$$

corresponding to a variation

$$\delta I = \int_{\mathcal{B}} \frac{\partial \mathcal{N}}{\partial \tau_k} \delta \tau_k dS,$$

for which cancellation is achieved by the adjoint boundary condition

$$\phi_k = \frac{\partial \mathcal{N}}{\partial \tau_k}.$$

Natural choices for \mathcal{N} arise from force optimization and

as measures of the deviation of the surface stresses from desired target values.

For viscous force optimization, the cost function should measure friction drag. The friction force in the x_i direction is

$$CD_{fi} = \int_B \sigma_{ij} dS_j = \int_B S_{2j} \sigma_{ij} d\mathcal{B}_\xi$$

so that the force in a direction with cosines n_i has the form

$$C_{nf} = \int_B n_i S_{2j} \sigma_{ij} d\mathcal{B}_\xi.$$

Expressed in terms of the surface stress τ_i this corresponds to

$$C_{nf} = \int_B n_i \tau_i dS,$$

so that basing the cost function (46) on this quantity gives

$$\mathcal{N} = n_i \tau_i.$$

Cancellation with the flow variation terms in equation (45) there for mandates an adjoint boundary condition

$$\phi_k = n_k.$$

Note that this choice of boundary condition also eliminates the first term in equation (45) so that it need not be included in the gradient calculation.

In the inverse design case, where the cost function is intended to measure the deviation of the surface stresses from some desired target values, a suitable definition is

$$\mathcal{N}(\tau) = \frac{1}{2} a_{lk} (\tau_l - \tau_{dl}) (\tau_k - \tau_{dk})$$

where τ_d is the desired surface stress. For cancellation

$$\phi_k \delta \tau_k = a_{lk} (\tau_l - \tau_{dl}) \delta \tau_k$$

This is satisfied by the boundary condition

$$\phi_k = a_{lk} (\tau_l - \tau_{dl}) \quad (47)$$

Assuming arbitrary variations in $\delta \tau_k$ this condition is also necessary.

In order to control the surface pressure and normal stress one can measure the difference

$$n_j \{ \sigma_{kj} + \delta_{kj} (p - p_d) \}$$

where p_d is the desired pressure. The normal component is then

$$\tau_n = n_k n_j \sigma_{kj} + p - p_d,$$

so that the measure becomes

$$\begin{aligned} \mathcal{N}(\tau) &= \frac{1}{2} \tau_n^2 \\ &= \frac{1}{2} n_l n_m n_k n_j \{ \sigma_{lm} + \delta_{lm} (p - p_d) \} \\ &\quad \cdot \{ \sigma_{kj} + \delta_{kj} (p - p_d) \}. \end{aligned}$$

This corresponds to setting

$$a_{lk} = m_l n_k$$

in equation (47). Defining the viscous normal stress as

$$\tau_{vn} = n_k n_j \sigma_{kj},$$

the measure can be expanded as

$$\begin{aligned} \mathcal{N}(\tau) &= \frac{1}{2} n_l n_m n_k n_j \sigma_{lm} \sigma_{kj} \\ &= \frac{1}{2} \tau_{vn}^2 + \tau_{vn} (p - p_d) + \frac{1}{2} (p - p_d)^2 \end{aligned}$$

For cancellation of the boundary terms

$$\begin{aligned} &\phi_k (n_j \delta \sigma_{kj} + n_k \delta p) \\ &= \{ n_l n_m \sigma_{lm} + n_l^2 (p - p_d) \} n_k (n_j \delta \sigma_{kj}) \end{aligned}$$

leading to the boundary condition

$$\phi_k = n_k (\tau_{vn} + p - p_d).$$

In the case of high Reynolds number this is well approximated by the equations

$$\phi_k = n_k (p - p_d), \quad (48)$$

which should be compared with the single scalar equation derived for the inviscid boundary condition (30). In the case of an inviscid flow, choosing

$$\mathcal{N}(\tau) = \frac{1}{2} (p - p_d)^2$$

requires

$$\phi_k n_k \delta p = (p - p_d) n_k^2 \delta p = (p - p_d) \delta p$$

which is satisfied by equation (48), but which represents an overspecification of the boundary condition since only the single condition (30) need be specified to ensure cancellation.

Boundary Conditions Arising from the Energy Equation

The boundary terms arising from the energy equation depends on the choice of temperature boundary condition at the wall. For the adiabatic case, the boundary contribution is (42)

$$\int_{\mathcal{B}} k \delta T \frac{\partial \Phi}{\partial n} d\mathcal{B}_{\xi}.$$

while for the constant temperature case the boundary term is (44)

$$\int_{\mathcal{B}} \Phi \left\{ \frac{S_{2j}}{J} \frac{\partial}{\partial \xi_2} \delta T + k \left[\delta \left(S_{2j} + \frac{S_{2j}}{J} \right) \frac{\partial T}{\partial \xi_l} \right] \right\} d\mathcal{B}_{\xi}.$$

One possibility is to introduce a contribution into the cost function which is dependent T or $\frac{\partial T}{\partial n}$ so that the appropriate cancellation would occur. However, since there is little physical intuition to guide the choice of such a cost function for aerodynamic design, an alternative solution is the set

$$\Phi = 0$$

in the constant temperature case or

$$\frac{\partial \Phi}{\partial n} = 0$$

in the adiabatic case. Note that in the constant temperature case, this choice of Φ on the boundary would also eliminate the boundary metric variation terms in (43).

Implementation of Navier–Stokes Design

The design procedures can be summarized as follows:

1. Solve the flow equations for ρ , u , v , p .
2. Smooth the cost function, if necessary.
3. Solve the adjoint equations for ψ subject to appropriate boundary conditions.
4. Evaluate \mathcal{G} .
5. Project \mathcal{G} into an allowable subspace that satisfies any geometric constraints.
6. Update the shape based on the direction of steepest descent.
7. Return to 1.

Practical implementation of the viscous design method relies heavily upon fast and accurate solvers for both the state (w) and co-state (ψ) systems. This work employs a well-validated Navier–Stokes solver developed by two of the authors [14]. The flow and adjoint equations are discretized using a semi-discrete finite volume scheme based on Jameson’s high resolution SLIP construction [15, 16, 17] and multi-stage Runge-Kutta time-stepping [18]. The preconditioned multigrid method developed by Pierce and Giles is used to accelerate the convergence of both flow and adjoint solvers [11, 12].

Results

Preconditioned Inverse Design

The first demonstration is an application of the preconditioning technique for inverse design with the Euler equations. The ONERA M6 (Fig. 2) wing is recovered for a lifting case starting from a wing with a NACA0012 section (Fig. 1) and using the ONERA M6 pressure distributions computed at $\alpha = 3.0$ and $M = 0.84$ as the target (Fig. 3). Thus, a symmetric wing section is to be recovered from an asymmetric pressure distribution. The calculations were performed on a $192 \times 32 \times 48$ C-H mesh with 294,912 cells. Each design cycle required 3 multigrid cycles for the flow solver using characteristic-based matrix dissipation with a matrix preconditioner and 12 multigrid cycles for the adjoint solver using scalar dissipation and a variable local time step (scalar preconditioner). Compared to a test in which the 3 multigrid cycles using the matrix preconditioner were replaced by 15 multigrid cycles using a standard scalar preconditioner, and 15 cycles were used in adjoint solver, each design cycle required about 3/8 as much computer time, while the number of design cycles required to reach the same level of error also fell from 100 to about 50. Use of the matrix preconditioner therefore reduced the total CPU time on an IBM 590 workstation from 97,683 sec (~ 27 hours) to 18,222 sec (~ 5 hours) for roughly equivalent accuracy.

Viscous Design

Due to the high computational costs of viscous design, a two-stage design strategy is adopted. In the first stage, a design calculation is performed with the Euler equations on a $192 \times 32 \times 48$ mesh to minimize the drag at a given lift coefficient by modifying the wing sections for a fixed planform. This results in a shock free wing at the design point.

In the second stage, the pressure distribution of the Euler solution is used as the target pressure distribution for inverse design with the Navier-Stokes equations on a $192 \times 64 \times 48$ mesh with 32 intervals normal to the wing concentrated inside the boundary layer region. Comparatively small modifications are required in the second stage, so that it can be accomplished with a small number of design cycles.

To test this strategy, an isolated wing representative of commercial aircraft in current use was used as the initial geometry. The design point was taken as a lift coefficient of 0.55 at a Mach number of 0.83. The initial wing exhibits a moderately strong shock across most of the upper surface, as can be seen in Fig. 4. In the first stage using the Euler equations, 60 design cycles were required to produce the shock free wing shown in Fig. 5, with an indicated drag reduction of 15 counts from 0.0196 to 0.0181. Viscous analysis with the Reynolds-averaged Navier-Stokes equations and a Baldwin-Lomax turbulence model at a Reynolds number of 12 million indicates that this wing still contains a weak shock due to the displacement effects of the boundary layer, as can be seen in Fig. 6. In the second stage of the design, 10 cycles using the Navier-Stokes equations were needed to recover the shock free wing shown in Fig. 7.

Conclusions

We have developed a three-dimensional control theory based design method for the Navier Stokes equations and successfully applied to the design of wings in transonic flow. The method represents an extension of our previous work on the design with the potential flow and Euler equations. The new method combines the versatility of numerical optimization methods with the efficiency of inverse design. The geometry is modified by a grid perturbation technique which is applicable to arbitrary configurations. The combination of computational efficiency with geometric flexibility provide a powerful tool, with the final goal being to create practical aerodynamic shape design methods for complete aircraft configurations.

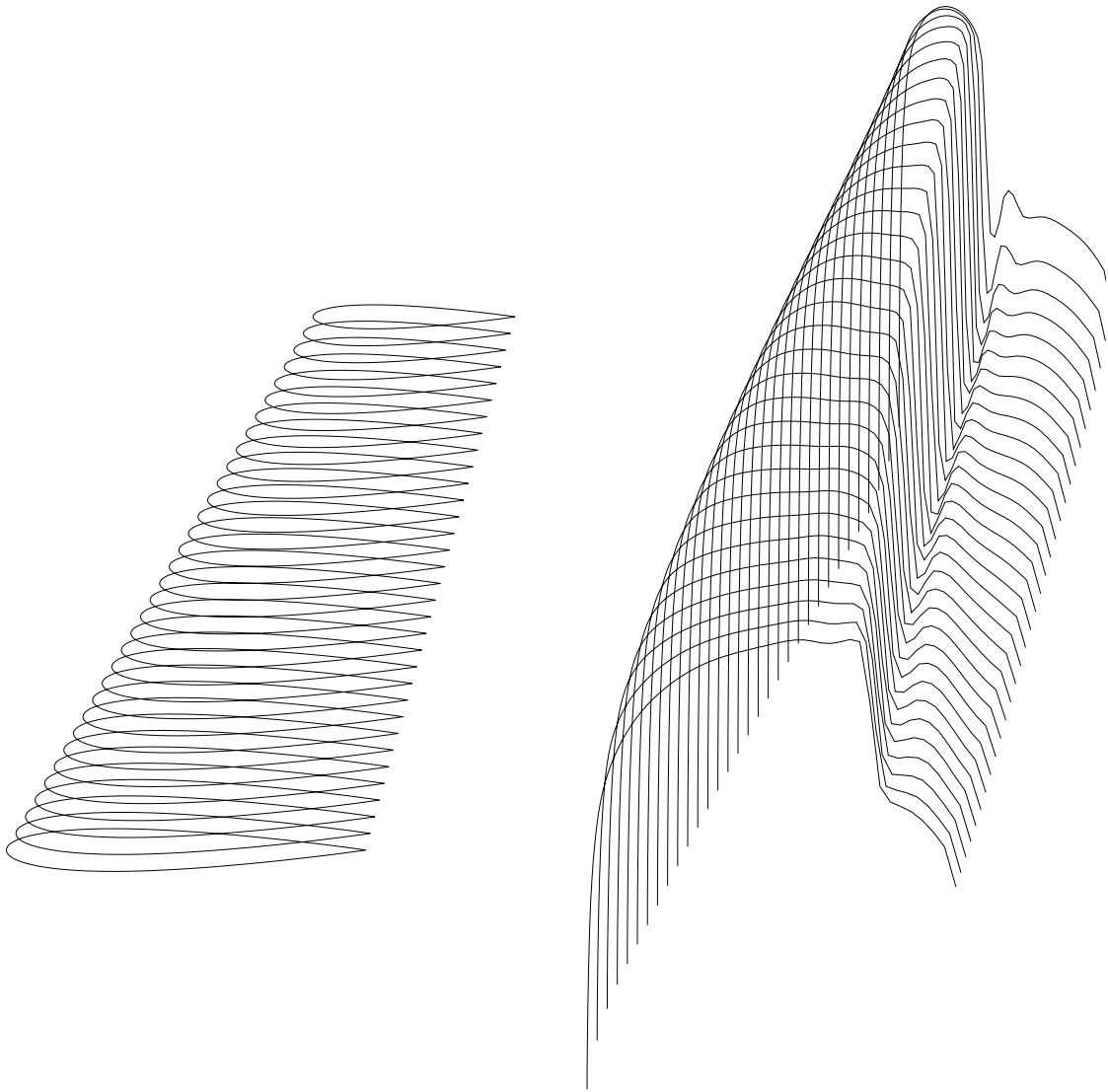
Acknowledgment

This work has benefited from the generous support of AFOSR under Grant No. AFOSR-91-0391, a NASA-IBM CRA grant and also the Rhodes Trust.

References

- [1] J.L. Lions. *Optimal Control of Systems Governed by Partial Differential Equations*. Springer-Verlag, New York, 1971. Translated by S.K. Mitter.
- [2] A. Jameson. Aerodynamic design via control theory. *J. Sci. Comp.*, 3:233–260, 1988.
- [3] A. Jameson. Optimum aerodynamic design using CFD and control theory. AIAA Paper 95-1729-CP, 1995.
- [4] A. Jameson. Automatic design of transonic airfoils to reduce the shock induced pressure drag. In *Proceedings of the 31st Israel Annual Conference on Aviation and Aeronautics, Tel Aviv*, pages 5–17, February 1990.
- [5] J. J. Reuther and A. Jameson. Control based airfoil design using the Euler equations. *AIAA paper 94-4272-CP*, 1994.
- [6] J. Reuther and A. Jameson. Aerodynamic shape optimization of wing and wing-body configurations using control theory. *AIAA paper 95-0123*, AIAA 33rd Aerospace Sciences Meeting, Reno, Nevada, January 1995.
- [7] J. Reuther, A. Jameson, J. Farmer, L. Martinelli, and D. Saunders. Aerodynamic shape optimization of complex aircraft configurations via an adjoint method. *AIAA paper 96-0094*, AIAA 34th Aerospace Sciences Meeting, Reno, Nevada, January 1996.
- [8] S. Ta'asan, G. Kuruwila, and M. D. Salas. Aerodynamic design and optimization in one shot. *AIAA paper 92-005*, 30th Aerospace Sciences Meeting and Exhibit, Reno, Nevada, January 1992.
- [9] O. Pironneau. *Optimal Shape Design for Elliptic Systems*. Springer-Verlag, New York, 1984.
- [10] O. Baysal and M. E. Eleshaky. Aerodynamic design optimization using sensitivity analysis and computational fluid dynamics. *AIAA Journal*, 30(3):718–725, 1992.
- [11] N.A. Pierce and M.B. Giles. Preconditioning compressible flow calculations on stretched meshes. AIAA Paper 96-0889, 34th Aerospace Sciences Meeting and Exhibit, Reno, NV, 1996.

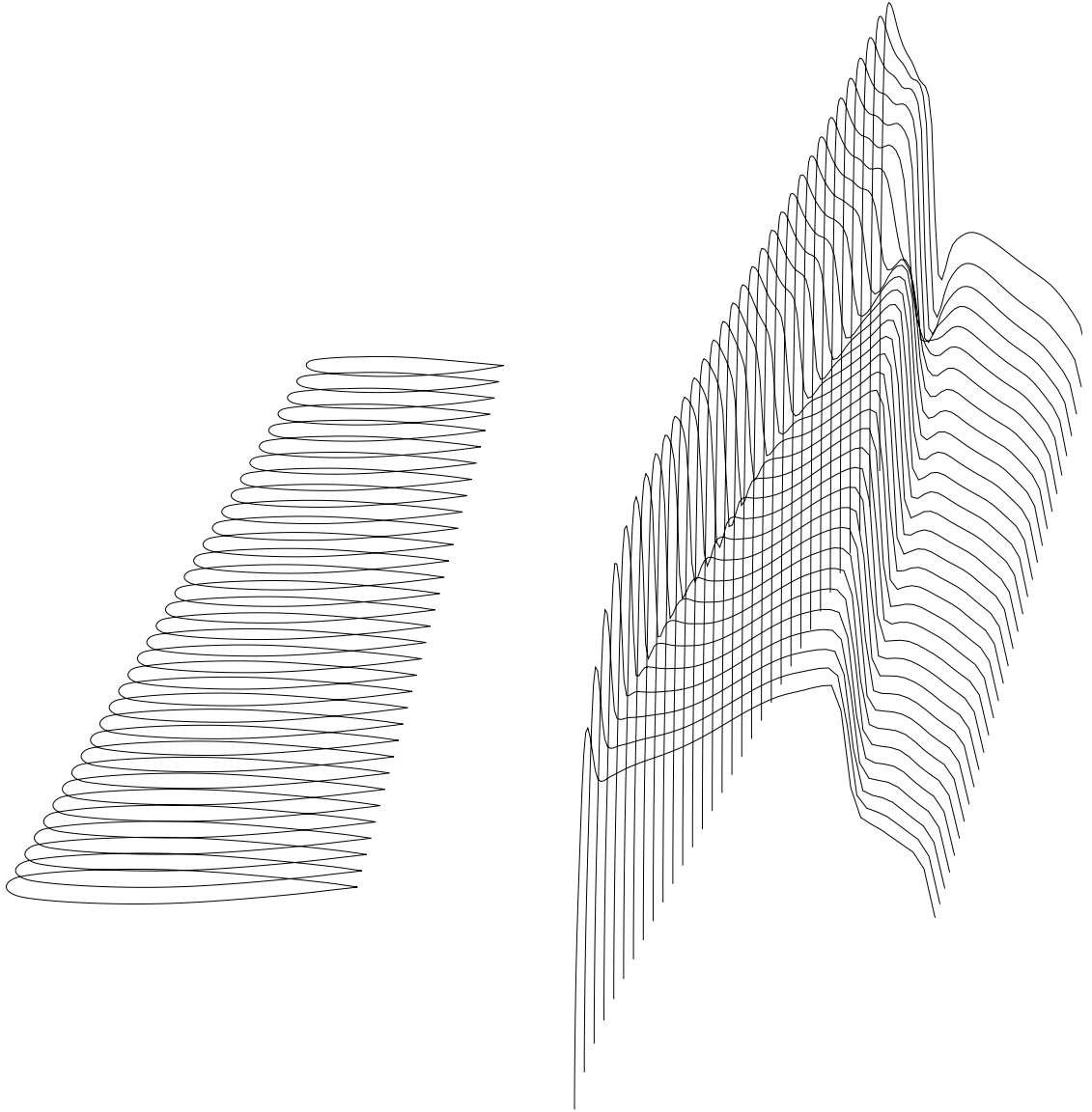
- [12] N.A. Pierce and M.B. Giles. Preconditioned multigrid methods for compressible flow calculations on stretched meshes. Submitted to *J. Comp. Phys.*, April, 1996.
- [13] A. Jameson. Optimum aerodynamic design using the Control Theory. *Computational Fluid Dynamics Review*, pages 495–528, 1995.
- [14] L. Martinelli and A. Jameson. Validation of a multigrid method for the Reynolds averaged equations. *AIAA paper 88-0414*, 1988.
- [15] A. Jameson. Analysis and design of numerical schemes for gas dynamics 1, artificial diffusion, upwind biasing, limiters and their effect on multigrid convergence. *Int. J. of Comp. Fluid Dyn.*, 4:171–218, 1995.
- [16] A. Jameson. Analysis and design of numerical schemes for gas dynamics 2, artificial diffusion and discrete shock structure. *Int. J. of Comp. Fluid Dyn.*, To Appear.
- [17] S. Tatsumi, L. Martinelli, and A. Jameson. A new high resolution scheme for compressible viscous flows with shocks. *AIAA paper 95-0466*, AIAA 33rd Aerospace Sciences Meeting, Reno, Nevada, January 1995.
- [18] A. Jameson, W. Schmidt, and E. Turkel. Numerical solutions of the Euler equations by finite volume methods with Runge-Kutta time stepping schemes. *AIAA paper 81-1259*, January 1981.



1a: Initial Wing.

1b: C_p on Upper Surface.

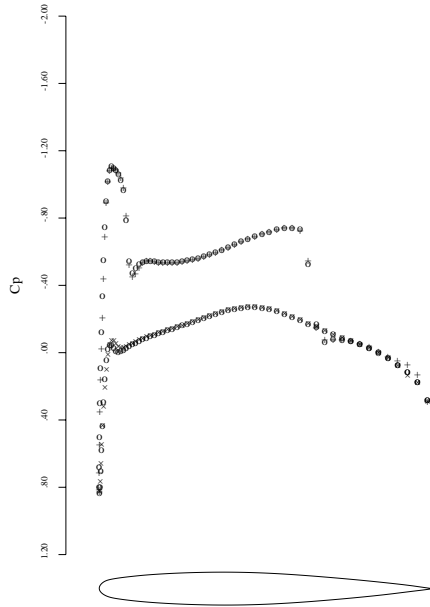
Figure 1: Inviscid Solution for Initial Wing (NACA 0012). $M = .84$, $C_l = .3000$, $C_d = .0205$, $\alpha = 2.935^\circ$.



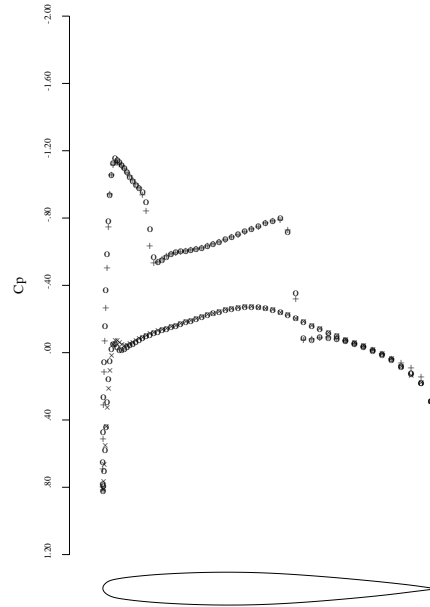
2a: Redesigned Onera M6 Wing.

2b: C_p on Upper Surface.

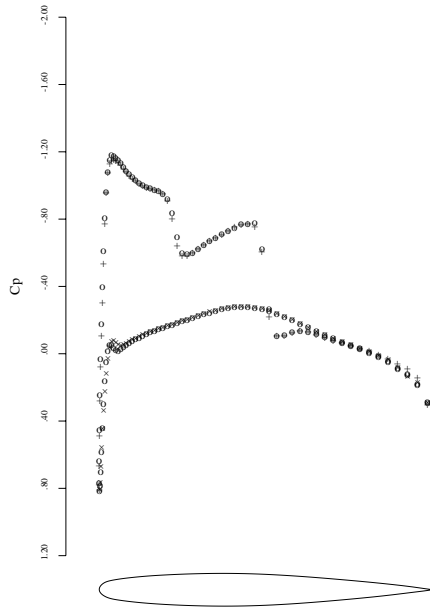
Figure 2: Solution for Redesigned Onera M6 Wing. $M = .84$, $C_l = .2967$, $C_d = .0141$, $\alpha = 2.935^\circ$



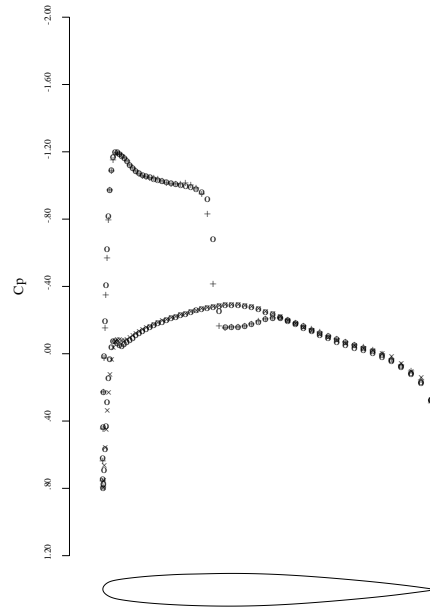
3a: span station $z = 0.297$



3b: span station $z = 0.484$

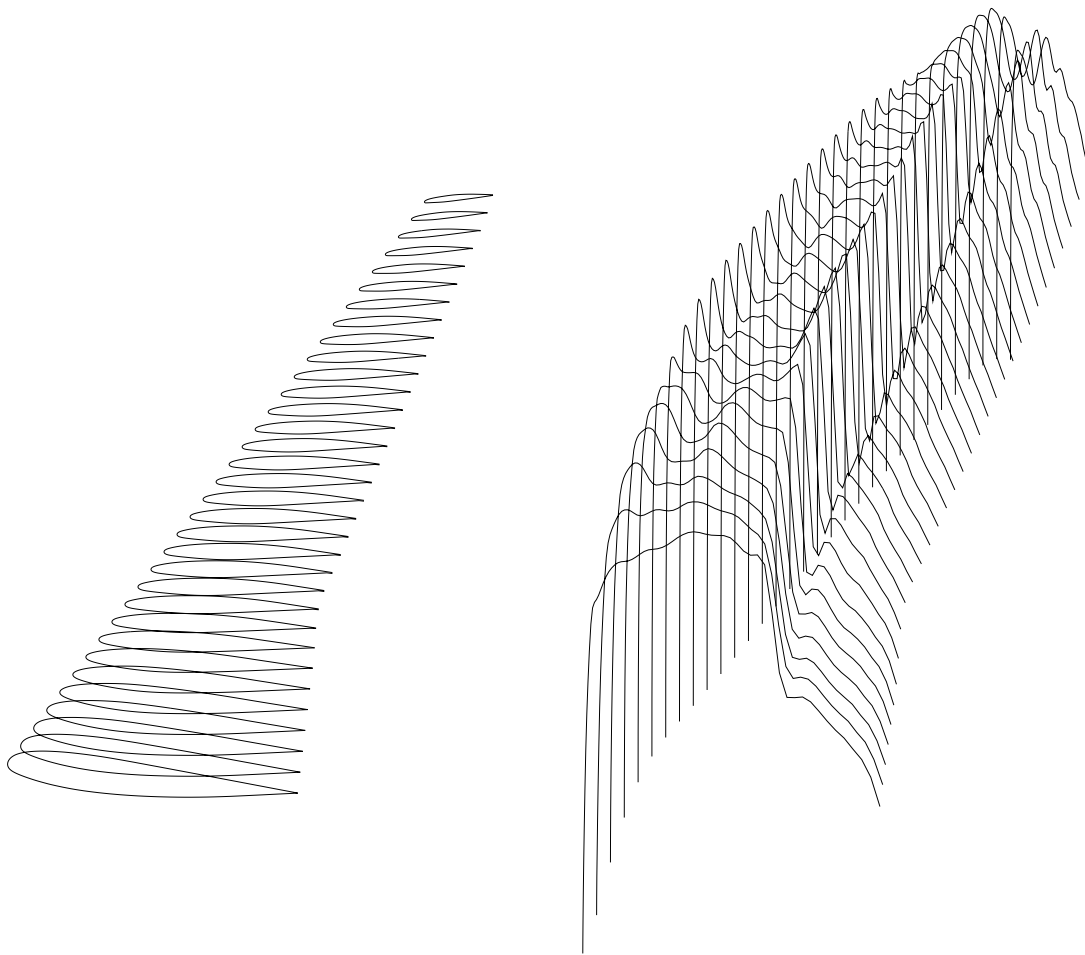


3c: span station $z = 0.672$



3d: span station $z = 0.859$

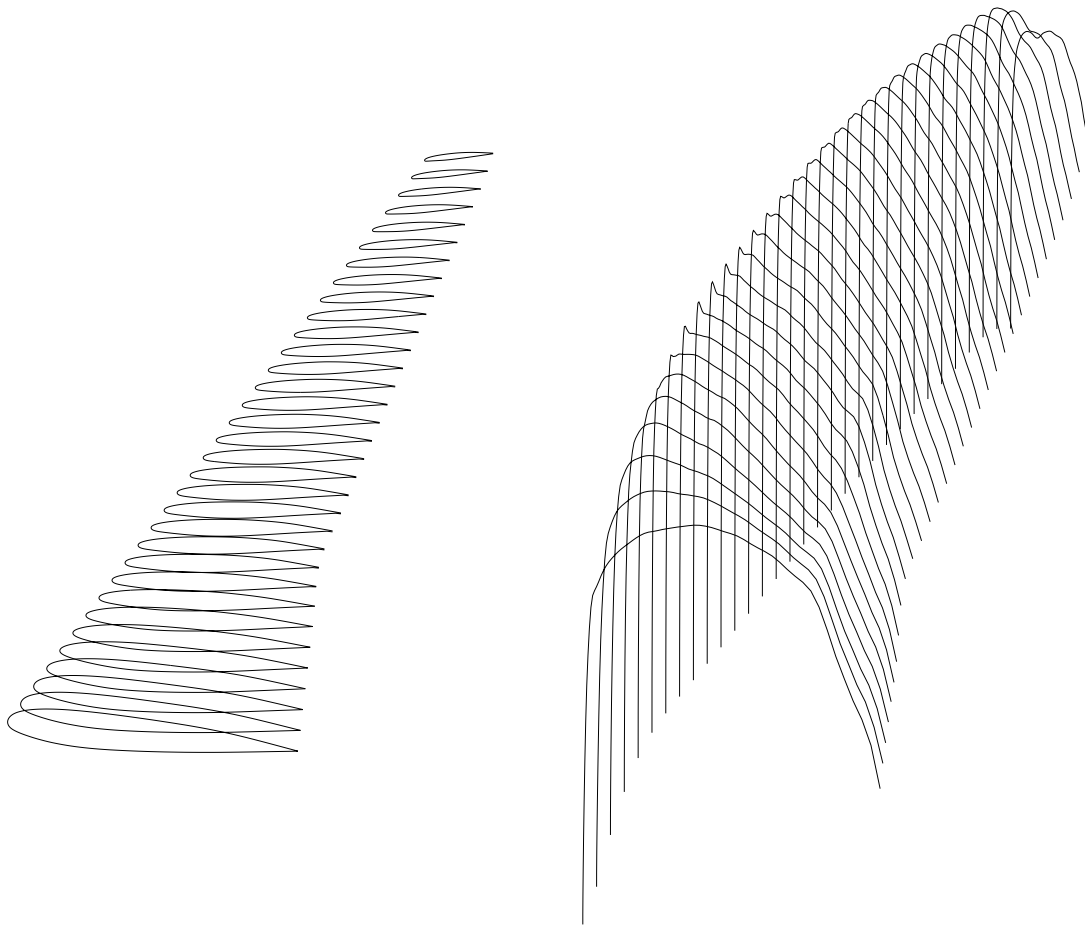
Figure 3: Target and Computed Pressure Distributions of Redesigned Onera M6 Wing. $M = 0.84$, $C_L = 0.2967$, $C_D = 0.0141$, $\alpha = 2.935^\circ$.



4a: Initial Wing.

4b: C_p on Upper Surface.

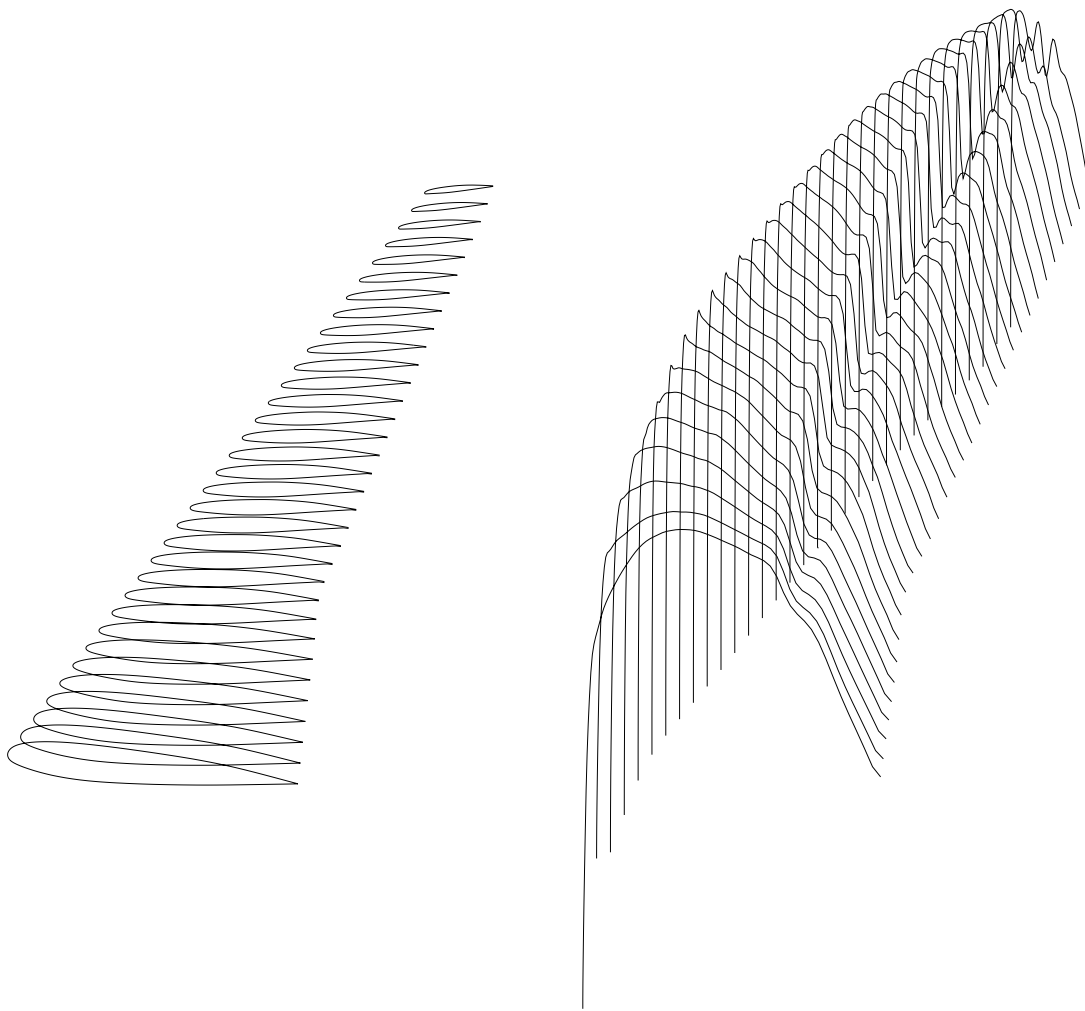
Figure 4: Inviscid Solution for Initial Wing. $M = .83$, $C_l = .5498$, $C_d = .0196$, $\alpha = 2.410^\circ$.



5a:
Wing After Inviscid Design.

5b: C_p on Upper Surface.

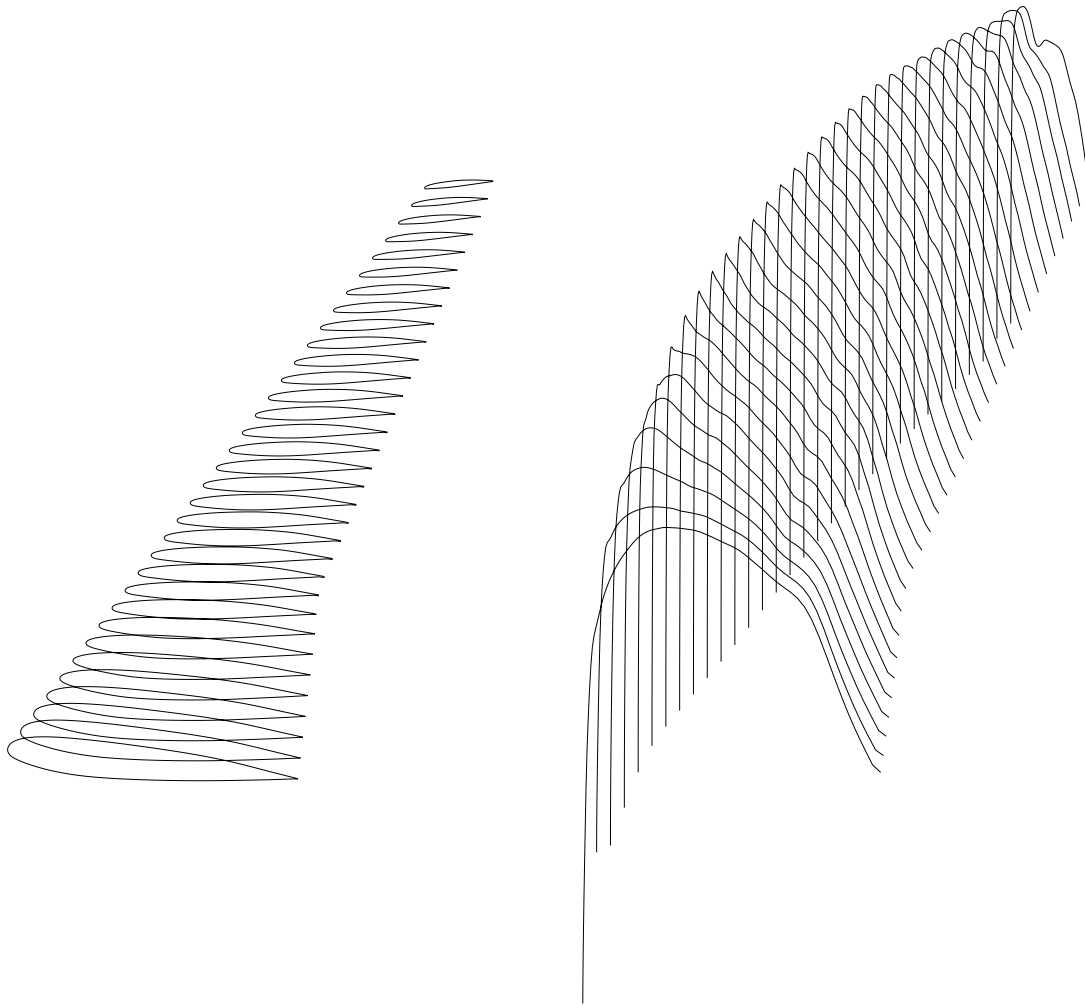
Figure 5: Stage 1: Inviscid Design. 60 Design Cycles in Drag Reduction Mode with Fixed Lift.
 $M = .83, C_l = .5500, C_d = .0181, \alpha = 1.959^\circ$.



6a: Wing After Inviscid Design.

6b: C_p on Upper Surface.

Figure 6: Viscous Solution for Inviscid Design. $M = 0.83$, $C_l = .5506$, $C_d = .0199$, $\alpha = 2.317^\circ$.



7a: Wing After Viscous Design.

7b: C_p on Upper Surface.

Figure 7: Stage 2: Viscous Re-design of Inviscid Design. 10 Design Cycles in Drag Reduction Mode with Fixed Lift.

$M = 0.83, C_l = .5508, C_d = .0194, \alpha = 2.355^\circ$.